Thermodynamic mixing of molecular states of the epidermal growth factor receptor modulates macroscopic ligand binding affinity

Michael R. HOLBROOK*[1], Linda L. SLAKEY† and David J. GROSS*[2]

*Program in Molecular and Cellular Biology, Department of Biochemistry and Molecular Biology, Lederle GRC, University of Massachusetts at Amherst, Amherst, MA 01003-4505, U.S.A, and †College of Natural Sciences and Mathematics, Lederle GRC, University of Massachusetts at Amherst, Amherst, MA 01003-4505, U.S.A.

The epidermal growth factor receptor (EGFr), when expressed on the cell surface, has long been known to display two distinct affinities for epidermal growth factor (EGF) binding. In addition, the treatment of cells expressing the EGFr with phorbol esters has been shown to cause a loss of the high-affinity binding capacity of the receptor. In the present study, point mutations that alter acidic or phosphorylation sites have been made in an intracellular domain near Tyr-992 (residues 988–992) of the EGFr. Equilibrium ^{125}I-EGF binding studies demonstrate that the conversion of Tyr-992 into glutamate induces a 4-fold decrease in the EGFr apparent low-affinity dissociation constant, whereas the mutation of two acidic residues, Asp-988 and Glu-991, or the conversion of Tyr-992 into phenylalanine does not alter EGFr affinity. Phorbol ester treatment of EGFr-expressing Chinese hamster ovary cells results in a loss of high-affinity binding and an increase in the apparent low-affinity dissociation constant of the receptor, similar to the effect of a truncation mutant in which the C-terminal 190 residues are deleted. These results are examined in the context of a new model for regulation of the affinity of the EGFr for EGF in which a cytosolic particle stabilizes the high-affinity conformation of the EGFr and a rapid equilibrium exists between EGFr high-affinity and low-affinity conformations. This model demonstrates that the macroscopic affinities of the EGFr can differ from the affinities of individual EGFr molecules and provides a theoretical framework whereby the measured affinities of the EGFr are modulated by intracellular interactions.

Key words: dissociation constant, equilibrium, ErbB family, signalling.

INTRODUCTION

The epidermal growth factor receptor (EGFr) is a 170 kDa cell-surface receptor that is a member of the ErbB family of signalling receptors. When expressed on the cell surface, the EGFr has been shown to possess two distinct affinities for binding epidermal growth factor (EGF) despite the fact that only one translation product of the EGFr gene is expressed [1]. The two affinities are typically invoked on the basis of Scatchard EGF binding plots that display a distinct concave upwards curvature. The high-affinity binding interaction is generally accepted to have a dissociation constant of less than 1 nM, whereas the low-affinity dissociation constant is 6–12 nM. High-affinity receptors comprise 1–10 % of the total receptor population, as shown by equilibrium binding in many cell types. The regulation of the affinity of the EGFr has been a topic of study for several years, yet the molecular mechanism responsible for the bimodal affinity has not been resolved. It is clear that the extracellular domain of the EGFr exhibits two distinct epitopes that are correlated with the two affinities of binding of EGF, on the basis of monoclonal antibody binding that can block either high-affinity or low-affinity EGF binding to the EGFr [2–5]. The means by which the EGFr presents these two ligand-binding sites has been discussed for many years.

Two types of model for explaining the heterogeneous affinities of the EGFr have been described: those based on extracellular regulation and those based on intracellular regulation. Clear evidence that complexes of EGF and a soluble extracellular EGFr domain interact to form dimers with altered EGF affinity was shown by Lemmon et al. [6], who also demonstrated that such interactions do not permit the concave-upwards Scatchard plots found for EGF binding to intact cells. A similar conclusion about the inability of receptor dimerization to explain the heterogeneous affinities of the EGFr was reached by Wofsy et al. [7]. It has been shown by Wiley [8] that increased receptor density can modulate the binding kinetics of EGF association and dissociation with the EGFr. Receptor density has also been suggested to have a role in the modulation of formation of EGFr dimers that have an altered ligand affinity compared with monomeric receptors [9]. However, invocation of this phenomenon can explain neither the small fraction of high-affinity EGFr of the total receptor pool found on cells nor the consistency with which heterogeneous affinities of EGF binding are seen on cells that express a range of EGFr densities.

Strong evidence exists that the intracellular domain of the EGFr has a key role in the regulation of extracellular EGF binding affinity. The role of the cytoplasmic tail of the EGFr in regulating receptor affinity has been studied by using a variety of deletion mutants, with somewhat conflicting results. Truncation of the C-terminus to residue 1126 resulted in the abolition of high-affinity binding [10], whereas deletion to residues 1060 [11] or 963 [12] did not affect ligand binding. An internal deletion of the putative actin-binding domain (residues 984–996) of the EGFr resulted in a decreased low-affinity dissociation constant of the EGFr, whereas the deletion of residues 921–940 abolished high-affinity binding [12].

Abbreviations used: CHO, Chinese hamster ovary; EGF, epidermal growth factor; EGFr, epidermal growth factor receptor; PKC, protein kinase C.

[1] Present address: Department of Pathology, University of Texas Medical Branch, Galveston, TX 77555-0609, U.S.A.
[2] To whom correspondence should be addressed at the Department of Biochemistry and Molecular Biology (e-mail dgross@biochem.umass.edu).

Further evidence of an intracellular mechanism for EGFr affinity regulation is found in published results in which the treatment of cells with phorbol ester abolished high-affinity EGF binding of the receptor via a mechanism that is not understood. Protein kinase C (PKC), which is activated by phorbol esters, phosphorylates the EGFr at Thr-654 [13,14], but phosphorylation at this residue is independent of the regulation of receptor affinity [14,15]. Thus serine or threonine phosphorylation of intracellular proteins other than the EGFr might be responsible for the modulation of EGFr affinity for EGF.

At least three different intracellular associations have been suggested to mediate the dual affinity states of the EGFr. Association of the EGFr with the cytoskeleton has been suggested to regulate the affinity of the EGFr on the basis of the finding that high-affinity EGFr associates preferentially with the cytoskeleton [16–18]. Dynamin, a GTPase that is required for the formation of clathrin-coated vesicles, associates with SH3-containing proteins as well as other membrane components [19]. Overexpression of a K44A mutant, catalytically inactive dynamin in HeLa cells eliminates the high-affinity population of EGFr [20], suggesting that overexpressed dynamin might sequester one or more EGFr-regulating proteins. Walker and Burgess [21] found that soluble, phosphorylatable cytoplasmic proteins function to regulate EGFr affinity. In that study, 3T3 fibroblast membrane preparations in which tyrosine kinases were activated were found to release phosphoproteins concomitant with the loss of high-affinity EGFr. The high-affinity state of the EGFr was reconstituted in the presence of alkaline phosphatase and released proteins, but not in the absence of either alone. These latter findings, in combination with new results presented here, form the basis of a new model of EGFr affinity regulation described in the present paper.

The essence of this model is that two separate extracellular conformations of the EGFr exist and that these conformations interact with EGF with distinctly different affinities. An intracellular molecule is postulated to trap a small fraction of the receptors in the high-affinity conformation, whereas the remainder of the receptors are found in dynamic equilibrium exchange between the high-affinity and low-affinity conformations. This exchange is the unique new feature of this model and is necessary to explain an enhanced affinity of the apparent (or macroscopic) low-affinity binding property of an EGFr with a point mutation at its most N-terminal tyrosine autophosphorylation site, Tyr-992. The cytosolic domain of the EGFr that has been shown to map to the actin-binding property of the receptor is coincident with this tyrosine autophosphorylation site [12,22,23]. Additionally, this short amino acid sequence is located close to the region of the receptor that targets activated EGFr for coated-pit-mediated internalization [24–26]. Recent work has shown that negatively charged residues within this domain slow the internalization rate of the EGF-bound EGFr [27]. The region around Tyr-992 is therefore a very active molecular interaction site that has a role in several aspects of EGFr function.

In the study presented here, specific point mutations have been made within residues 984–996 of the EGFr, and an examination of the role of this region in regulation of ligand binding affinity has been undertaken. These mutations have demonstrated that negative charge at residue 992, an SH2 binding site in the wild-type receptor, enhances the affinity of the EGFr for EGF, whereas alteration in other negatively charged sites within this domain has no effect on ligand binding affinity. Additionally, a truncation mutant has shown that a domain within the C-terminal 190 residues of the EGFr is necessary for the regulation of the affinity of the EGFr. The domain responsible for the phorbol-ester-induced loss of receptor affinity has also been localized to the C-terminal 190 residues of the EGFr.

EXPERIMENTAL

Cell lines

Chinese hamster ovary (CHO) cells of the CHO-K1 subline and A431 cells were purchased from the American Type Culture Collection (Manassas, VA, U.S.A.). CHO cells expressing the wild-type EGFr were a gift from Roger Davis (University of Massachusetts Medical Center, Worcester, MA, U.S.A.) [14,15].

Cell culture

CHO cells do not express detectable levels of endogenous EGFr and were therefore an excellent choice for the expression of EGFr in these studies. All CHO cell lines were maintained in Ham's/F12 nutrient medium (Gibco, Grand Island, NY, U.S.A.) supplemented with 5% (v/v) fetal bovine serum (Summit Biotechnology, Fort Collins, CO, U.S.A.) (complete medium). The generation of the site-directed EGFr mutants and transfection of CHO cells has been described previously [27]. A431 cells, which are of human epidermoid carcinoma origin, were used as a control because they endogenously express approx. 10^6 EGFr on their cell surfaces. These cells were maintained in DMEM (Dulbecco's modified Eagle's medium) (Gibco) with 5% (v/v) fetal bovine serum. All cells were maintained in a humidified 37 °C incubator in air/CO_2 (19:1).

Binding assays

Cells were plated in 48-well polystyrene tissue culture plates at a density of 10^4 cells per well in 0.5 ml of complete medium. The cells were allowed to grow for 3 days at 37 °C in air/CO_2 (19:1). Before EGF binding experiments, the cells were serum-starved in Ham's/F12 medium alone for 24 h. Three wells were treated with trypsin and the cell number per well was determined. The medium for other wells was replaced with cold serum-free Ham's/F12 and the plates were pre-chilled at 4 °C for at least 20 min before the initiation of each experiment to block receptor internalization. For experiments with PMA (Sigma Chemical Co., St Louis, MO, U.S.A.), cells were treated with 10 nM PMA for 30 min at 37 °C before being chilled and, subsequently, during the pre-chill.

Medium was aspirated from the pre-chilled wells and replaced with 50 μl of binding medium consisting of Ham's/F12 medium supplemented with 0.1% BSA (Sigma) and containing various concentrations of mouse EGF (Harlan Bioproducts, Indianapolis, IN, U.S.A.) plus ^{125}I-EGF (Amersham, Arlington Heights, IL, U.S.A.). Each assay was performed in triplicate wells. The concentrations of EGF added ranged from 16.3 pM to 24.45 nM. ^{125}I-EGF was used alone up to 0.815 nM, then non-radioactive EGF was added to this amount of ^{125}I-EGF in the remaining samples to complete the required mass of ligand. Cells were incubated with EGF at 4 °C for at least 6 h to allow binding to reach equilibrium. The EGF-containing solution was then removed from each well to a 10 mm × 75 mm polypropylene tube. The cells were washed twice with approx. 250 μl of ice-cold PBS and the washes were added to the polypropylene tube, which was counted as the unbound fraction. The cells were then solubilized with 250 μl of ice-cold 0.62 M NaOH for 2–3 min; this sample plus a single 0.5 ml ice-cold PBS wash were removed to a polypropylene tube and counted as the bound fraction of EGF. Samples were counted for 5 min in a gamma counter. The results presented are averages of at least three experiments.

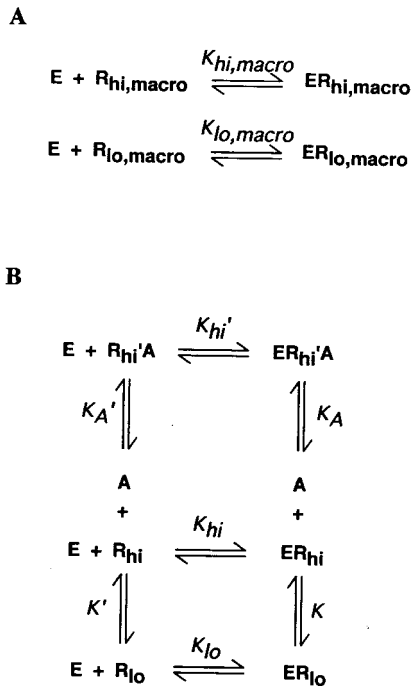

Scheme 1 Standard two-site (A) and ternary complex (B) models of EGFr affinity regulation

The ternary complex model employs particle A, which is in limiting concentration, trapping a fraction of the total number of EGFr in the high-affinity binding conformation [(**B**), top complexes]. The remaining EGFr are in equilibrium exchange, producing a mixed macroscopic dissociation constant with a value between those of the molecular K_{hi} and K_{lo} conformations [(**B**), bottom pair of coupled reactions].

Data analysis

^{125}I-EGF equilibrium binding data was analysed with two different binding schemes. The first, a standard published approach used to analyse equilibrium ligand binding, assumed two independent, saturable types of EGF binding sites on each cell line (Scheme 1A). Each type of site had a distinct EGF dissociation constant and number of sites per cell. Given the definitions R_{hi}, R_{lo}, $K_{hi,macro}$ and $K_{lo,macro}$ for, respectively, the numbers of binding sites of high and low affinity and the dissociation constants for these sites, the expression relating total EGF binding to the concentration of EGF ([E]) is:

$$\text{Bound} = \frac{R_{hi}}{1+\frac{K_{hi,macro}}{[E]}} + \frac{R_{lo}}{1+\frac{K_{lo,macro}}{[E]}}. \quad (1)$$

The second binding model (Scheme 1B) employed a modified ternary complex system similar to, but extended beyond, that analysed by Mayo et al. [28]. The chief difference between the model of Mayo et al. and that presented here lies in a rapid interconversion between the two conformations of the EGFr that correspond to low and high affinity of the receptor for EGF. This interconversion, with equilibrium constant K, results in a macroscopic apparent low-affinity dissociation constant of the interconverting mixture of receptors that assumes a value between the molecular dissociation constants of the two EGFr conformations. This thermodynamic mixing of states produces a macroscopic low-affinity dissociation constant that can vary as a function of K. This capability was found necessary to accommodate an elevated macroscopic low-affinity dissociation constant found for one of the EGFr mutants. Further development of the biological basis of this ternary complex EGFr binding model is given in the Discussion section.

Conservation of mass of EGFr and particle A requires that:

$$\left.\begin{aligned} &R_t = [R_{hi}]+[R_{lo}]+[R_{hi}'A]+[ER_{hi}]+[ER_{lo}]+[ER_{hi}'A] \\ &\text{and} \\ &A_t = [A]+[R_{hi}'A]+[ER_{hi}'A] \end{aligned}\right\} \quad (2)$$

where R_t and A_t are the total numbers of EGFr and A particles per cell, and square brackets represent the concentrations of species shown in Scheme 1(B). The equilibrium dissociation constants in Scheme 1(B) are defined as:

$$\left.\begin{aligned} &K_{hi}' = \frac{[E][R_{hi}'A]}{[ER_{hi}'A]},\ K_{hi} = \frac{[E][R_{hi}]}{[ER_{hi}]},\ K_{lo} = \frac{[E][R_{lo}]}{[ER_{lo}]} \\ &K_A = \frac{[A][ER_{hi}]}{[ER_{hi}'A]},\ K = \frac{[ER]_{lo}}{[ER_{hi}]},\ K_A' = \frac{[A][R_{hi}]}{[R_{hi}'A]} = K_A\frac{K_{hi}}{K_{hi}'} \\ &\text{and}\ \ K' = \frac{[R_{lo}]}{[R_{hi}]} = K\frac{K_{lo}}{K_{hi}} \end{aligned}\right\} \quad (3)$$

In these expressions, [E] is the concentration of free EGF in the medium, which is assumed to be constant for all experiments. This was confirmed by direct measurement (results not shown). The last two relations in eqns (3) show explicitly that the dissociation constants within each cyclic reaction pathway are coupled.

From eqns (2) and (3) the expression relating free and bound EGF for this model is:

$$\text{Bound} = \frac{R_t - A_t - k + S}{2(a+bK)} \left\{ 1+K+\frac{A_t}{\frac{c}{2(a+bK)}(R_t - A_t - k + S)+K_A} \right\} \quad (4)$$

where symbols are defined as above and in Scheme 1 with the following additional definitions:

$$S = \sqrt{(R_t + A_t + k)^2 - 4R_tA_t},\ k = K_A\frac{a+bK}{c},$$

$$a = 1+\frac{K_{hi}}{[E]},\ b = 1+\frac{K_{lo}}{[E]} \text{ and } c = 1+\frac{K_{hi'}}{[E]}.$$

Each of the dissociation constants represents the actual time-averaged molecule–molecule interaction between species; thus the dissociation constants are molecular. For the EGF–EGFr dissociation constants, each can be ascribed to a distinct extracellular conformation of the EGFr. As will be discussed more fully below, the bottom reaction cycle in Scheme 1(B) mixes the two EGFr dissociation constants for the high-affinity and low-affinity conformations of the receptor, with the result that a single macroscopic dissociation constant of intermediate value is detected in an equilibrium binding experiment. Because two states collapse into one blended state within this model, it is not possible to distinguish between the high-affinity EGFr conformation that is bound to particle A and the high-affinity conformation that is not. For this reason, in what follows, the assumption is made that these two conformations are identical. The mathematical consequences of this assumption are that $K_{hi}' = K_{hi}$, $K_A' = K_A$ and $c = a$.

The difficulty or ease with which EGF equilibrium binding data can be analysed in the context of this ternary complex model depends on the quality of the data and the underlying biochemical properties of the system. Most cell lines that express EGFr have only a small number of measurable high-affinity binding sites. In the ternary complex model shown in Scheme 1(B), this indicates that a small population of occupied binding sites represents the fraction of receptors bound to A particles. Thus the parameters of the model related to this fraction, A_t and K_A, are difficult to extract with a high degree of accuracy from the data. This intrinsic property of the biochemical system, which places a similar constraint on R_{hi} and $K_{hi,macro}$ in the two-independent-site model (Scheme 1A), will be seen in the high uncertainties for these parameters in the analysis that follows.

Binding data in the form bound versus [EGF] were fitted to each of the models by using a Marquardt–Levenberg least-squares technique implemented in IGOR Pro (Wave Metrics, Lake Oswego, OR, U.S.A.). All ^{125}I-EGF data fits employed both bound and unbound fractions. After correction for dilution with unlabelled EGF and calibration against a standard curve, the non-specific binding of ^{125}I-EGF was calculated by fitting the four highest EGF concentration data points to a two-site model in which the non-specific site was assigned a dissociation constant of 1 M and the number of sites per cell was allowed to vary. Subsequent analysis employed this low-affinity binding as a fixed pair of parameters that represented the non-specific EGF binding in each experiment. The two chief advantages of this approach over the more common use of a very large excess of unlabelled ligand are that the non-specific binding is measured at concentrations of EGF much closer to those used in the experiment and much less ligand is required. The former advantage ensures that non-specific binding with a multiplicity of affinities are sampled at ligand concentrations internally consistent with those used in any given experiment.

The standard two-site model parameters were fitted directly; all four free parameters (two dissociation constants and two receptor surface concentrations) were allowed to vary freely. The ternary complex model was fitted iteratively, first with all parameters (four dissociation constants, total receptor number and total number of particles A) allowed to vary, then with all parameters except the conversion constants K and K_A [the dissociation constant for the EGFr and the associated particle (Scheme 1B)] allowed to vary freely. A second independent fit of the ternary complex model held the molecular high-affinity and low-affinity dissociation constants K_{hi} and K_{lo} fixed at 0.001 and 20 nM respectively, with all other parameters allowed to vary freely. This fit was done to determine whether the EGF binding properties of all mutant EGFr were consistent with the idea that all EGFr constructs displayed an identical pair of extracellular conformational states responsible for the molecular dissociation constants, with variations in the macroscopic, mixed-state dissociation constants due to changes in the extent of EGFr interconversion and interaction with particle A.

RESULTS

Ligand binding

The role of negative charges in the vicinity of Tyr-992 in the EGFr intracellular domain in modulation of EGFr internalization has been described [27]. The role of these charges in modulation of EGFr affinity for EGF is examined here. In brief, four specific mutations were made at positions that are at or near the most N-terminal of the tyrosine autophosphorylation sites within the EGFr. Two of these mutants, Asp-988 → Asn (D988N) and Glu-991 → Gln (E991Q), convert negatively charged amino acids into their uncharged analogues. Two mutations also were made at Tyr-992. One converted the tyrosine residue into phenylalanine (Y992F) to mimic the uncharged state of non-phosphorylated Tyr-992; the second conversion was into a glutamic residue (Y992E) to mimic the negative charge resulting from the phosphorylation of Tyr-992.

In addition, a truncation mutation was produced while generating the E991Q mutants. This mutation truncated the EGFr after Gln-996 (E991Qt$_{996}$), which removes 190 residues from the C-terminus of the receptor.

^{125}I-EGF equilibrium binding studies were performed on cell lines that expressed the various mutant EGFr. In addition, experiments were performed on CHO cells expressing the wild-type EGFr, A431 cells endogenously expressing wild-type EGFr, and untransfected control CHO cells expressing undetectable levels of EGFr. The results generated in the binding experiments were fitted to a binding model that assumed the existence of two independent populations of EGFr, each with a distinct affinity for EGF. This is the standard model used by most authors to analyse EGFr binding affinity. This fitting routine calculated the receptor number for both the high-affinity and low-affinity populations as well as the corresponding dissociation constants as described in eqn (1). The results for each of the cell lines, with the exception of E991Qt$_{996}$ (see below) and untransfected CHO cells (which showed no detectable specific EGF binding; results not shown), demonstrated that the wild-type and mutant receptors displayed two distinct populations with different affinities for EGF (Table 1). Variation between experiments was large in some instances, particularly in the number of receptors per cell and in the high-affinity dissociation constant. The former was due largely to variability in the numbers of cells plated in each experiment; this variability did not affect the determination of dissociation constants or the relative numbers of high-affinity and low-affinity sites. The latter was to be expected because only a small amount of ^{125}I-EGF was bound to the population of receptors that displayed a high affinity for EGF. Statistical analysis indicated that only the Y992E mutant EGFr displayed significantly different values of the low-affinity dissociation constant (95% confidence level) and the high-affinity dissociation constant (90% confidence level) in comparison with wild-type EGFr.

Scatchard analyses of representative experiments for the wild-type EGFr and the E991Q, E991Qt$_{996}$ and Y992E mutant EGFr are shown in Figure 1. To put these experiments on the same plot, each data set was scaled relative to its fitted number of total receptors, i.e. all binding data were scaled to a maximum relative binding of 1. The differences in the slopes of the Scatchard plots reflect the differences between high-affinity and low-affinity K_d values and relative numbers of high-affinity and low-affinity binding sites for each experiment. Also plotted in Figure 1 are the curves derived from the fits for each of the data sets. Included are the fits to the standard two-site model as described above, along with two fits to the ternary complex model as described below. In all cases except one of the E991Qt$_{996}$ ternary complex fits, the curves align very well with the data points.

These results suggest that EGF–EGFr binding properties are unaffected by point mutations near Tyr-992 that alter negative charges, with the exception of Tyr-992 → Glu. The addition of a permanent negative charge at residue 992 increased the apparent affinity of the receptor 4-fold for the dominant low-affinity population of receptors; this result is statistically significant at the 95% confidence level by a t test. The high-affinity population also displayed an increased affinity for EGF, although this result is not significant at the 95% confidence level, due primarily to the relatively small number of high-affinity sites in cells expressing

Table 1 ^{125}I-EGF binding to cells expressing wild-type and mutant EGFr

^{125}I-EGF equilibrium binding data for A431 and CHO cells expressing wild-type and mutant EGFr. The data were fitted to a standard two-affinity binding model as described in the text. Receptor number per cell and dissociation constants are given for both the high-affinity (R_{hi}, $K_{hi,macro}$) and low-affinity (R_{lo}, $K_{lo,macro}$) interactions as well as the percentage of total receptors that were of high affinity. Values for number of receptors and K_d are shown as means ± S.D. for fit values from n experiments on each cell line. Dissociation constants that were significantly different, on the basis of a t test, from those of wild-type EGFr expressed in CHO cells are denoted as follows: $^*P < 0.1$; $^{**}P < 0.05$.

Receptor	n	$10^5 \times R_{lo}$	$K_{lo,macro}$ (nM)	$10^3 \times R_{hi}$	$K_{hi,macro}$ (nM)	Proportion high affinity (%)
A431	4	13 ± 2	5.7 ± 0.7	5 ± 5	0.02 ± 0.02	0.4
Wild-type	6	8 ± 9	6.0 ± 1.8	20 ± 17	0.07 ± 0.05	2.5
D988N	4	1.6 ± 1.1	6.7 ± 3.0	5.2 ± 2.1	0.09 ± 0.04	3.1
E991Q	5	2.0 ± 1.1	5.2 ± 1.7	8.8 ± 4.0	0.06 ± 0.05	4.4
E991Qt$_{996}$	3	2.2 ± 1.7	20 ± 10	0.09 ± 0.13	0.19 ± 0.23	0.04
Y992E	3	0.8 ± 0.2	1.6 ± 0.8**	1.7 ± 1.0	0.01 ± 0.01*	2.1
Y992F	5	4.2 ± 1.7	6.5 ± 2.2	11 ± 6	0.11 ± 0.10	2.5

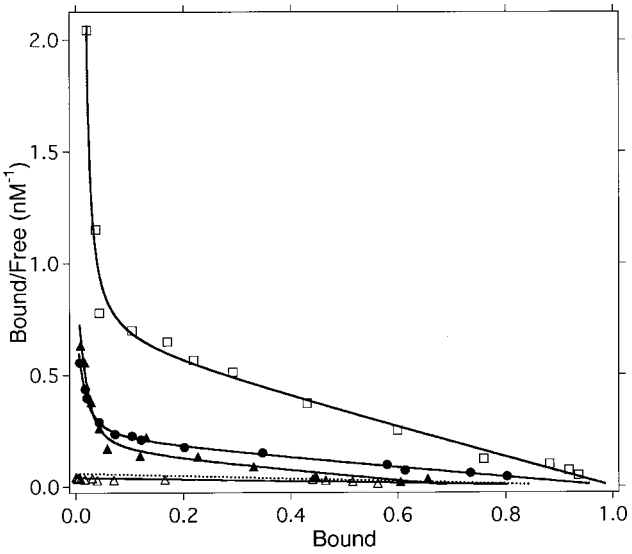

Figure 1 Scatchard plots of ^{125}I-EGF binding to EGF receptors as expressed on the surfaces of CHO cells

Included are data points from individual experiments for the wild-type (●), Y992E (□), E991Q (▲) and E991Qt$_{996}$ (△) EGFr. Smooth curves are fits to the standard two-site model (solid lines), the ternary complex model with all parameters allowed to vary (broken lines) and the ternary complex model with the high-affinity and low-affinity dissociation constants held fixed at 0.001 and 20 nM respectively (dotted lines). Fits to each model are indistinguishable within the thickness of the lines except for one of the fits to the E991Qt$_{996}$ data, thus most broken and dotted lines are not visible in the plot.

wild-type and mutant EGFr. Thus an increased negative charge at Tyr-992 induced a strong shift of the low-affinity dissociation constant of the EGFr towards a higher affinity.

Ternary complex model

In the context of the standard model of EGF–EGFr interaction, the above results imply that a novel extracellular conformation of the EGFr was produced by the point mutation Y992E. This inference is necessary because the standard model provides no mechanism whereby the measured, macroscopic affinities of binding of EGF can be modulated other than by direct alteration of the extracellular domain of the receptor. This seems implausible, particularly because there is no other published evidence suggesting that the several molecular interactions known to involve Tyr-992 induce such a conformational change. An alternative model for the EGF–EGFr interaction has therefore been examined; this model invokes only the two wild-type extracellular conformations of the EGFr and yet is capable of predicting the observed shift of the low-affinity dissociation constant for the Y992E receptor as well as the non-linear Scatchard plots found for EGF–EGFr binding.

Scheme 1(B) shows the ternary complex model for the regulation of EGFr binding affinity. This model incorporates three molecules: EGF, the EGFr and a third accessory molecule A. The function of the accessory molecule is to trap a subset of EGFr that are in the high-affinity conformation. This interaction is governed by dissociation constant K_A. Those receptors that are not trapped by particle A are free to interconvert between the high-affinity and low-affinity conformations. This exchange between affinity conformations, governed by the equilibrium constant K, results in a single macroscopic dissociation constant that is intermediate between the actual molecular dissociation constants K_{hi} and K_{lo}. Such equilibrium mixing, driven by simple thermodynamic energetics, does not occur in the standard model for EGFr binding because the high-affinity and low-affinity conformations are explicitly independent of each other and therefore do not interconvert. It is this equilibrium mixing step, in combination with the trap for the high-affinity conformation of the EGFr, that makes this ternary complex model capable of describing the behaviour of wild-type and mutant EGFr, including Y992E. The key element in this model compared with other models is the rapid interconversion of EGFr between the high-affinity and low-affinity conformations. This mixing produces a macroscopic, observable 'low' affinity for EGF that lies between the actual molecular affinities K_{hi} and K_{lo} of the two receptor conformations. The macroscopic 'high' affinity for EGF is identical with the molecular affinity of the high-affinity conformation in the model as described here, although a simple extension of the model to include conformation interconversion for the A·EGFr complex would permit the model to generate a mixed macroscopic 'high'-affinity dissociation constant as well. Because the mixed-state 'low'-affinity dissociation constant obscures the two dissociation constants for the high-affinity and low-affinity conformations of the receptor, it is not possible in this model, when applied to equilibrium binding data, to distinguish between K_{hi} and K_{hi}' of Scheme 1(B). Lacking any evidence that three independent EGFr extracellular conformations exist, binding data are interpreted here as arising from two independent EGFr extracellular conformations, i.e. $K_{hi} = K_{hi}'$. Thus, in the context of this ternary complex model, macroscopic binding experiments report two apparent affinities for EGF–EGFr binding, one of which represents a blend between two interconverting receptor conformations. To keep these

Table 2 ^{125}I-EGF binding to cells expressing wild-type and mutant EGFr fitted to the ternary complex model

^{125}I-EGF equilibrium binding data fitted to the ternary complex model for A431 and CHO cells expressing wild-type and mutant EGFr. The ternary complex model employs the total number of receptors per cell (R_t), the total number of A sites per cell (A_t), the molecular dissociation constants for the high-affinity and low-affinity conformations of the receptor (K_{hi} and K_{lo} respectively), the dissociation constant for A (K_A in sites per cell) and a conversion constant K (see Scheme 1). Values for these parameters are shown as mean ± S.D. for fitted values from n experiments on each cell line. Dissociation constants that were significantly different, on the basis of a t test, from those of wild-type EGFr expressed in CHO cells are denoted as follows : $^*P < 0.1$; $^{**}P < 0.05$. The E99Qt$_{996}$ fits were not all convergent.

Receptor	n	$10^5 \times R_t$	$10^3 \times A_t$	K_{lo} (nM)	K_{hi} (nM)	$10^3 \times K_A$	K
A431	4	13 ± 2	5 ± 5	7 ± 1	0.02 ± 0.02*	10 ± 20	100 ± 200
Wild-type	6	8 ± 9	20 ± 20	8 ± 2	0.04 ± 0.02	0.4 ± 0.5	3.9 ± 0.2
D988N	4	2 ± 1	5 ± 2	8 ± 4	0.05 ± 0.06	0.2 ± 0.2	3.8 ± 0.4
E991Q	5	2 ± 1	9 ± 4	7 ± 2	0.02 ± 0.01*	0.2 ± 0.2	4.0 ± 0.3
E991Qt$_{996}$	3	2 ± 2	30 ± 20	20 ± 10	4 ± 3	3000 ± 1000*	3.1 ± 0.4*
Y992E	3	0.8 ± 0.2	2 ± 1	2 ± 1**	0.001 ± 0.001**	0.1 ± 0.1	3.8 ± 0.2
Y992F	5	4 ± 2	20 ± 20	8 ± 3	0.05 ± 0.06	0.5 ± 0.8	3.9 ± 0.3

Table 3 ^{125}I-EGF binding to cells expressing wild-type and mutant EGFr fitted to the ternary complex model with fixed K_{lo} and K_{hi}

^{125}I-EGF equilibrium binding data fitted to the ternary complex model for A431 and CHO cells expressing wild-type and mutant EGFr. This fit of the ternary complex model varied the total number of receptors per cell (R_t), the total number of A sites per cell (A_t), the dissociation constant for A (K_A in sites per cell) and the conversion constant K (see Scheme 1). For this fit the molecular high-affinity and low-affinity dissociation constants, K_{hi} and K_{lo}, were fixed at 0.001 and 20 nM respectively. Values for R_t, A_t, K_A and K are shown as means ± S.D. for fitted values from n experiments on each cell line. Dissociation constants that were significantly different, on the basis of a t test, from those of wild-type EGFr expressed in CHO cells are denoted as follows : $^*P < 0.1$; $^{**}P < 0.05$.

Receptor	n	$10^5 \times R_t$	$10^3 \times A_t$	$10^3 \times K_A$	K
A431	4	13 ± 2	5 ± 5	3 ± 3	0.4 ± 0.1
Wild-type	6	8 ± 9	20 ± 20	5 ± 5	0.5 ± 0.2
D988N	4	2 ± 1	5 ± 2	1.4 ± 0.4	0.6 ± 0.4
E991Q	5	2 ± 1	9 ± 4	1.5 ± 0.8	0.4 ± 0.1
E991Qt$_{996}$	3	2 ± 2	30 ± 50	2000 ± 2000	4 ± 3
Y992E	3	0.8 ± 0.2	2 ± 1	0.3 ± 0.4*	0.09 ± 0.05**
Y992F	5	4 ± 2	11 ± 6	4 ± 3	0.5 ± 0.3

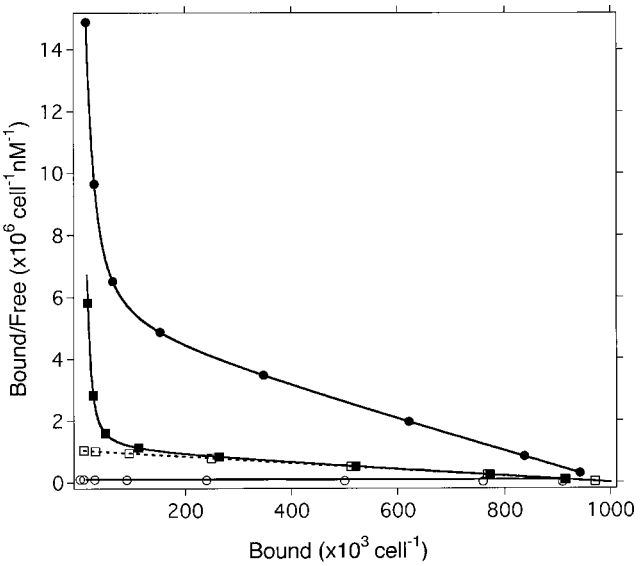

Figure 2 Scatchard plots of synthetic data created from the ternary complex model and fits to the two-site model

Synthetic data were generated to mimic the wild-type EGFr (■), the Y992E mutant EGFr (●), PMA-treated or E991Qt$_{996}$ truncated receptor (○) and EGFr for which binding to the A particle had been decreased (□). The synthetic data were fitted to the standard two-independent-site model; fits for each data set are shown by solid or broken lines.

concepts separate in what follows, the true molecular dissociation constants that result from direct molecule–molecule interactions at the cell surface are referred to as K_{hi} and K_{lo} for the high-affinity and low-affinity EGFr conformations as shown in Scheme 1(B). The macroscopic, observed high-affinity and low-affinity dissociation constants are termed $K_{hi,macro}$ and $K_{lo,macro}$ respectively. Because the functional form of the binding equation for the ternary complex model [eqn (4)] is different from that for the standard model for two independent sites, it is not possible to derive a general relationship between $K_{lo,macro}$, K_{hi} and K_{lo}. However, when minimal binding between the EGFr and particle A occurs, i.e. when K_A approaches infinity, eqn (4) reduces to a form identical with that of a standard single-site binding isotherm:

$$\text{Fraction bound} = \frac{[EGF]}{[EGF] + K_{lo,macro}} \quad (5)$$

where $K_{lo,macro} = (K_{hi} + KK_{lo})/(1 + K)$. Similarly, in the limit where binding between the EGFr and particle A becomes very strong, i.e. when K_A approaches zero, $K_{hi,macro}$ can be shown to equal K_{hi}.

Two separate applications of the ternary complex model were used to analyse the ^{125}I-EGF binding data for wild-type and mutant EGFr. The first allowed all parameters in the model to vary during the data fitting (Table 2). The second restricted K_{hi} and K_{lo} to fixed values of 0.001 and 20 nM respectively for all cell lines. This restricted fitting was done to determine whether all the wild-type and mutant receptor binding results were consistent with a model in which precisely two affinity-defining conformations of the EGFr, which were present for all mutant receptors, could account for the varied macroscopic binding constants seen for the various cell lines. Table 3 shows the ternary complex model parameter values for the fit in which K_{hi} and K_{lo} were held fixed; in all cases this restricted form of the ternary complex model fitted all wild-type and mutant receptors (Figure 1). Only the Y992E mutant displayed K and K_A values that were significantly different from those of the wild-type receptor for this latter fitting. Based on the premise of the model, this result suggests that the Tyr-992 → Glu mutation alters the interconversion equilibrium between the high-affinity and low-affinity conformations of the EGFr.

Table 4 Parameters used for generation and returned from fitting of synthetic binding data

Four sets of parameters (R_t, A_t, K_{lo}, K_{hi}, K_A and K) were used to generate synthetic EGF binding data from the ternary complex model as plotted in Figure 2. These data were then fitted to a standard two-site binding model, for which the returned parametric values (R_{lo}, R_{hi}, $K_{lo,macro}$ and $K_{hi,macro}$) are shown. The ternary complex input parameters were chosen to simulate four situations : normal (wild-type), equilibrium mixing, favouring the high-affinity conformation (Y992E), decreased binding of particle A to the EGFr, concomitant with equilibrium mixing favouring the low-affinity conformation (PMA/truncation), and decreased binding of particle A to the EGFr with normal mixing of the low-affinity and high-affinity conformations (increased K_A).

Parameter	Wild-type	Y992E	PMA/truncation	Increased K_A
$10^5 \times R_t$	10	10	10	10
$10^3 \times A_t$	20	20	20	20
K_{lo} (nM)	20	20	20	20
K_{hi} (nM)	0.001	0.001	0.001	0.001
K_A	10	10	10^7	10^7
K	0.05	0.01	1	0.05
$10^5 \times R_{lo}$	9.8	9.8	9.9	10
$10^3 \times R_{hi}$	20	20	12	0.04
$K_{lo,macro}$ (nM)	0.95	0.20	10.0	0.95
$K_{hi,macro}$ (nM)	0.001	0.001	9.4	0.14

Table 5 ^{125}I-EGF equilibrium binding data for PMA-treated CHO cells expressing wild-type and mutant EGFr

Data were fitted to a standard two-site binding model as described in the text. The number of receptors expressed on the cell surface and dissociation constants are given for both the high-affinity (R_{hi}, $K_{hi,macro}$) and low-affinity (R_{lo}, $K_{lo,macro}$) interactions as well as the percentage of total receptors that were of high affinity. Values for numbers of receptors and K_d are shown as means $\pm$ S.D. for fit values from n experiments on each cell line. None of the dissociation constants were significantly different from those of PMA-treated wild-type EGFr expressed in CHO cells. Dissociation constants that were significantly different, on the basis of a t test, from those of the same mutant EGFr expressed in untreated CHO cells are denoted as follows : $^*P < 0.1$; $^{**}P < 0.05$.

Receptor	n	$10^5 \times R_{lo}$	$K_{lo,macro}$ (nM)	$10^3 \times R_{hi}$	$K_{hi,macro}$ (nM)	Proportion high affinity (%)
Wild-type	3	4 ± 1	14 ± 5	4 ± 2	0.10 ± 0.02	1
D988N	3	1.9 ± 0.9	$19 \pm 4^{**}$	0.2 ± 0.3	0.05 ± 0.04	0.1
E991Q	3	0.8 ± 0.8	$9 \pm 2^*$	0.5 ± 0.7	0.1 ± 0.1	0.6
E991Qt$_{996}$	2	0.1 ± 0.2	20 ± 10	0.004 ± 0.004	5 ± 3	0.08
Y992E	4	2 ± 1	$7.8 \pm 0.9^{**}$	1 ± 1	2 ± 3	0.5
Y992F	4	2 ± 2	$11 \pm 3^*$	0.3 ± 0.6	7 ± 11	0.02

As noted above, the functional dependence on [EGF] of the ternary complex model is very different from that of the standard two-site model, yet both models generate remarkably similar binding curves. To explore the relationship between the parameters of the ternary complex model (R_t, A_t, K_{hi}, K_{lo}, K_A and K) and those of the two-site model (R_{hi}, $K_{hi,macro}$, R_{lo}, $K_{lo,macro}$), synthetic binding data were calculated with the ternary complex model [eqn (4)] with four sets of parameters intended to mimic a wild-type EGFr, the Y992E and E991Qt$_{996}$ mutant receptors, and a receptor for which binding to the A particle of the ternary complex model is disrupted. As noted below, EGFr from PMA-treated cells have binding properties similar to those of the E99Qt$_{996}$ mutant, so these receptors could be modelled with the same parameters. These synthetic data are shown as data points in Figure 2. The synthetic data were then fitted with the standard two-site model [eqn (1)], with results shown by the smooth curves in Figure 2. The parameters that were used to generate the synthetic data and the values returned from the fits to the two-site model are given in Table 4. These results illustrate five features of the ternary complex model. First, it is capable of producing binding data that closely mimic those of the standard two-site model. Secondly, the macroscopic low-affinity $K_{lo,macro}$ returned by the standard two-site model is intermediate between the molecular dissociation constants K_{hi} and K_{lo}. Thirdly, a change in the equilibrium mixing constant K to favour the high-affinity conformation decreases the macroscopic low-affinity dissociation constant $K_{lo,macro}$. Fourthly, a decrease in affinity between the EGFr and A particle decreases R_{hi} and increases $K_{hi,macro}$ to values near that of $K_{lo,macro}$, i.e. high-affinity binding disappears. Lastly, increases in both K and K_A are necessary to decrease both high-affinity binding and increase $K_{lo,macro}$, a situation found for the E991Qt$_{996}$ mutant and for PMA-treated cells.

PMA-treated cells

The treatment of wild-type EGFr-expressing cells with phorbol esters has long been known to decrease the number of high-affinity EGF binding sites on the cell surface. To determine whether the above mutations within the EGFr altered the response of the receptors to phorbol esters, equilibrium binding studies were performed on EGFr-expressing cells in the presence of PMA. For all cell lines, mutant and wild-type, the treatment of EGFr-expressing CHO cells with PMA decreased the number of high-affinity EGF binding sites to a significant extent. Table 5 gives the parameter values from the standard two-site model fit; Table 6 gives values for the ternary complex model with K_{hi} and K_{lo} held fixed at 0.001 and 20 nM respectively. For the standard model fit, the fraction of sites that are of high affinity decreased for all PMA-treated CHO cell lines in comparison with untreated cells except the E991Qt$_{996}$ mutant. The parameter values in Table 5 also suggest that a decrease of 1.5–3-fold in receptor affinity for its ligand after treatment with PMA is statistically significant for the low-affinity receptor population in most mutant EGFr. It seems likely that PMA treatment of CHO cells expressing wild-type and mutant EGFr induces a concomitant loss of high-affinity binding sites and a decrease in binding affinity for the low-affinity sites. In the context of the ternary complex model, this suggests that fewer EGFr are trapped in the complex with

Table 6 ^{125}I-EGF binding to PMA-treated cells expressing wild-type and mutant EGFr fitted to the ternary complex model with fixed K_{lo} and K_{hi}

This fit of the ternary complex model varied the total number of receptors per cell (R_t), the total number of A sites per cell (A_t), the dissociation constant for A (K_A in sites per cell) and the conversion constant K (see Scheme 1). For this fit the dissociation constants for the high-affinity-defining and low-affinity-defining extracellular conformations of the receptor, K_{hi} and K_{lo}, were fixed at 0.001 and 20 nM respectively. Values for R_t, A_t, K_A and K are shown as means ± S.D. for fit values from n experiments on each cell line. None of the dissociation constants were significantly different from those of PMA-treated wild-type EGFr expressed in CHO cells. Only the Y992F mutant receptor had a significantly different mixing dissociation constant K (t test, $P < 0.1$) when comparing untreated and PMA-treated cells; all other dissociation constants for mutant and wild-type receptors were not significantly different from the values for untreated cells.

Receptor	n	$10^5 \times R_t$	$10^3 \times A_t$	$10^3 \times K_A$	K
Wild-type	3	4 ± 1	4 ± 2	1.0 ± 0.8	5 ± 6
D988N	3	1.9 ± 0.8	2 ± 2	1500 ± 1400	30 ± 40
E991Q	3	0.8 ± 0.8	6 ± 5	2000 ± 2000	0.8 ± 0.3
E991Qt$_{996}$	2	2 ± 2	7 ± 10	2000 ± 2000	40 ± 60
Y992E	4	2 ± 1	100 ± 100	1000 ± 2000	1.3 ± 0.3
Y992F	4	2 ± 2	200 ± 200	1000 ± 1000	1.7 ± 0.9

particle A and that the equilibrium mixing of the molecular high-affinity and low-affinity conformations is shifted towards the low-affinity conformation. This notion is borne out by the ternary complex model parameters in Table 6 in which the K and K_A dissociation constants are all larger than the corresponding values for untreated cells in Table 3. Similarly, the data simulations of Figure 2 and Table 4 support the same conclusion.

DISCUSSION

Ligand binding to the full-length point mutant EGFr described here indicates that, of the point mutants made, only the Y992E mutation affects EGF binding. This mutation induces a decrease in both the high-affinity and low-affinity macroscopic dissociation constants of the EGFr. Although statistically (at the 90% confidence level) the high-affinity macroscopic dissociation constant seems to be smaller, this conclusion is arguable primarily owing to the small number of high-affinity binding sites present and the inherent difficulty in obtaining an accurate measurement of their binding properties in the presence of a large amount of low-affinity binding. However, the decrease in the macroscopic low-affinity dissociation constant of the Y992E mutant in comparison with the wild-type EGFr seems to be a real effect. In the context of the standard view of EGF binding to its receptor, this result implies that a point mutation in the cytoplasmic domain of the receptor has altered the extracellular conformation of the receptor that is responsible for low-affinity binding. This view is problematic because it necessarily invokes a coupling between intracellular and extracellular conformational changes in the EGFr molecule and additionally requires the EGFr to adopt at least three distinct extracellular conformations.

An alternative view of this phenomenon is that intracellular interactions of the EGFr are responsible for shifts in the apparent extracellular affinity of the EGFr and that changes in the normal high-affinity and low-affinity EGFr conformations are not necessary. The extended ternary complex model shown in Scheme 1 employs these features and has been shown to be capable of describing, in a self-consistent fashion, EGF binding for the collection of mutant and wild-type receptors with and without PMA treatment that were studied here (Figure 1, Tables 2, 3 and 6). In support of this model, Walker and Burgess [21] have shown that high-affinity binding sites of the EGFr, previously down-modulated by ligand activation, can be reconstituted in a cell-free system, suggesting that a third particle forms a ternary complex with EGF and the EGFr for receptors that express the high-affinity conformation.

The inclusion of a second cyclic reaction pathway in which the molecular high-affinity and low-affinity conformations of the EGFr can mix with each other (Scheme 1B, bottom reaction cycle) is necessary in the model because binding data from the Y992E EGFr point mutant described here, along with a deletion mutant described by van der Heyden et al. [12], suggest that the apparent dissociation constant for low-affinity EGF binding can be modulated by mutations within the intracellular domain of the receptor. Rather than attempting to explain the observed changes in the extracellular binding properties of the EGFr by conformational or other interactions conveyed across the plasma membrane, which would necessitate a multiplicity of extracellular EGFr conformations, this model invokes an intracellular explanation for this phenomenon. If there are two, and only two, distinct conformations of the EGFr that interact with EGF, i.e. the molecular high-affinity and low-affinity conformations, and if these two conformations can interconvert, then thermodynamics will force the EGFr system to exhibit an apparent intermediate affinity for EGF for those receptors that are free to interconvert. In the model of Scheme 1(B), these are the receptors that are not trapped by interaction with the ternary particle A. Modulation of this apparent macroscopic affinity, which is lower than that of the trapped, molecular high-affinity conformation and higher than that of the molecular low-affinity conformation, can be accomplished by altering the extent to which the molecular high-affinity and low-affinity conformations can interconvert. This interconversion is regulated via the conversion constant K (Scheme 1B). The multiple steps involved in these interconversions are undetectable in equilibrium binding assays and become apparent in kinetic experiments probing the time-dependent changes in EGF binding only on a perturbation in binding conditions such as step changes in EGF concentration. Multiple rate constants corresponding to the several reaction steps would be present for this sort of affinity regulatory system. We and other workers have shown that multiple kinetic-rate constants are found for the EGF–EGFr interaction [28–30], which demonstrates that multiple reaction pathways underlie the regulation of the EGF–EGFr interactions. The application of the ternary complex model to kinetic binding of EGF to cells will require careful data collection and analysis of a set of coupled differential equations containing from 8 to 14 rate constants, which is beyond the scope of the work presented here.

The ternary complex model described here is capable of predicting a continuum of macroscopic EGF dissociation constants while postulating only two EGFr conformations with fixed, distinct molecular affinities for EGF. This aspect of the model predicts that an EGF-blocking antibody specific for the low-affinity conformation of the receptor would shift the macroscopic low-affinity dissociation constant to K_{hi}, thus increasing the apparent number of high-affinity sites in a macroscopic

binding experiment, the latter increase arising from the complement of receptors in the high-affinity conformation that are not bound to particle A. Such a result was found for the monoclonal antibody 2E9 [3]. In contrast, an EGF-blocking antibody specific for the high-affinity conformation would shift the macroscopic low-affinity dissociation constant to K_{lo} while obliterating all high-affinity macroscopic binding. This was found for monoclonal antibody 108, in which $K_{lo,macro}$ increased from 14 to 22 nM for 3T3 cells expressing human EGFr [2].

Treatment of EGFr-expressing cells with PMA causes a loss of high-affinity EGF binding in all of the point mutants described here and an increase in the $K_{lo,macro}$ of the low-affinity EGF interaction (Table 5). This result can be understood from the modified ternary complex model. If Ser/Thr phosphorylation of either particle A or of the EGFr reduces the interaction between A and the receptor, i.e. increases the dissociation constant K_A in the model of Scheme 1(B), the extent of trapping of the EGFr in the A-bound high-affinity conformation would decline. This prediction is borne out by experiment. The phosphorylation of an unknown soluble factor has been shown to abolish the high-affinity EGF–EGFr interaction, with a restoration of high-affinity binding on dephosphorylation [21]. Phosphorylation activation of a competitor for either A or the EGFr would also accomplish a similar effect. Further, a phosphorylation-induced increase in the interconversion constant K would shift the high-affinity and low-affinity mixing equilibrium toward the molecular low-affinity conformation, thus decreasing the macroscopic low-affinity ligand binding. As expected, shifts in K and K_A towards larger values are seen for the PMA-treated cell data when fitted to the ternary complex model (Table 6). Similarly, simulations of EGF binding demonstrated the same effect (Figure 2 and Table 4). Thus the ternary complex model with equilibrium mixing of the molecular high-affinity and low-affinity conformations of the receptor seems consistent with all the data and is amenable to a simpler molecular interpretation than is possible with the standard model of EGF–EGFr binding.

The E991Qt$_{996}$ mutant, in addition to the Glu 991 → Gln point mutation, is truncated after Gln-996. This truncation causes a nearly complete loss of the high-affinity binding capacity for EGF in addition to a 3-fold increase in the macroscopic low-affinity $K_{lo,macro}$ compared with the wild-type and E991Q receptors. Thus this truncation mutation makes the receptor equivalent to a full-length receptor from PMA-treated cells. Similar results have been seen in a truncation of the C-terminal 63 residues [10]. These results suggest that the C-terminal 190 residues of the EGFr contain a structural determinant for maintaining the high-affinity 'state' of the receptor, which, in the ternary complex model, would be an interaction site for particle A as well as the regulatory site responsible for interconversion of the population of EGFr that are not bound to particle A. The lack of effect of PMA treatment on EGFr binding properties for the E991Qt$_{996}$ mutant is consistent with the idea that the region of the EGFr that is responsible for regulating the phorbol-ester-activated PKC-induced loss of high affinity of the EGFr lies within the C-terminal 190 residues of the receptor. The only known PKC phosphorylation site on the EGFr is Thr-654; the phosphorylation of this residue has been shown to be independent of receptor affinity [14,15]. It therefore seems as though the effect of phorbol ester involves a second cellular protein that is PKC-phosphorylated. It also seems as though this protein interacts with the EGFr in the C-terminal 190 residues or that this protein, when phosphorylated, acts to disrupt the interaction of this portion of the EGFr with some other molecule. In the context of the ternary complex model shown in Scheme 1(B), this PKC-phosphorylated protein could be particle A or it could displace the EGFr from particle A. This hypothesis is consistent with the results of Walker and Burgess [21], who demonstrated that an EGFr-associated protein, when phosphorylated, dissociated from the receptor simultaneously with the loss of high-affinity EGF binding and, when dephosphorylated, restored high-affinity binding.

The deletion of residues 921–940 has been shown to produce a loss of high-affinity binding capacity of the EGFr [12]. This sequence has been suggested to be the region of the receptor that determines the high-affinity binding of the EGFr with EGF [12]; however, its presence in the deletion mutants that do not produce high-affinity receptors (E991Qt$_{996}$ shown here) [10] suggests that it alone does not confer high-affinity ligand binding capacity. It might be that residues 921–940 interact with the C-terminal 190 residues of the EGFr to enable the high-affinity conformation of the receptor or that residues 921–940 form an additional binding site for particle A.

Interestingly, the deletion of residues 984–996 of the EGFr produces a 3-fold increase in ligand binding affinity of the low-affinity class of receptor according to the standard two-site model [12]. This result is similar to that seen in the Y992E mutant. These results suggest that Tyr-992, or residues near it, have a key role in regulating the affinity distribution of the EGFr by altering the interconversion mixing of the true high-affinity and low-affinity conformations of the receptor via the dissociation constant K in Scheme 1(B).

The binding of EGF to the EGFr has been a facet of receptor biology that has long been under study. The full-length EGFr presents itself with two well-defined affinities for EGF when expressed on the cell surface. In this study it is shown that an increase in the low-affinity interaction of the EGFr with EGF is evidence for a point mutant EGFr that mimics the charge of phosphorylated Tyr-992. In addition, the truncation of the EGFr to Gln-996 causes a loss of high-affinity ligand binding and eliminates the effect of phorbol esters on ligand binding. These results demonstrate that Tyr-992 and the C-terminal 190 residues of the EGFr are involved in the determination of the EGFr affinity for EGF. This study also demonstrates that phorbol-ester-induced PKC regulation of EGFr affinity for EGF occurs through the C-terminal 190 residues of the receptor, most probably by the phosphorylation of a cytosolic partner protein that interacts with the EGFr near its C-terminus.

We thank Dr Julia Hill for assistance with one of the Y992E ligand binding experiments, Mr John O'Donnell for assistance in clone isolation for the Y992E CHO cell line, and Dr Robert Weis for reading the manuscript. These studies were supported in part by American Cancer Society grant FRA-437, National Science Foundation grant MCB-9304393 and United States Department of Agriculture NRI Competitive Grant 99-35203-8679 (to D. J. G.). Any opinions, findings and conclusions or recommendations expressed in this material are those of the authors and do not necessarily reflect the views of the funding organizations.

REFERENCES

1 Yarden, Y. and Ullrich, A. (1988) Molecular analysis of signal transduction by growth factors. Biochemistry **27**, 3113–3119
2 Bellot, F., Moolenaar, W., Kris, R., Mirakhur, B., Verlaan, I., Ullrich, A., Schlessinger, J. and Felder, S. (1990) High-affinity epidermal growth factor binding is specifically reduced by a monoclonal antibody, and appears necessary for early responses. J. Cell Biol. **110**, 491–502
3 Defize, L. H. K., Boonstra, J., Meisenhelder, J., Tertoolen, L. G. J., Tilley, B. C., Hunter, T., van Bergen en Henegouwen, P. M. P., Moolenaar, W. H. and de Laat, S. W. (1989) Signal transduction by epidermal growth factor occurs through the subclass of high affinity receptors. J. Cell Biol. **109**, 2495–2507
4 Gregoriou, M. and Rees, A. R. (1984) Properties of a monoclonal antibody to epidermal growth factor receptor with implications for the mechanism of action of EGF. EMBO J. **3**, 929–937

5 Kawamoto, T., Sato, J. D., Le, A., Polikoff, J., Sato, G. H. and Mendelsohn, J. (1983) Growth stimulation of A431 cells by epidermal growth factor: identification of high-affinity receptors for epidermal growth factor by an anti-receptor monoclonal antibody. Proc. Natl. Acad. Sci. U.S.A. **80**, 1337–1341
6 Lemmon, M. A., Bu, Z., Ladbury, J. E., Zhou, M., Pinchasi, D., Lax, I., Engelman, D. M. and Schlessinger, J. (1997) Two EGF molecules contribute additively to stabilization of the EGFR dimer. EMBO J. **16**, 281–294
7 Wofsy, C., Goldstein, B., Lund, K. and Wiley, H. S. (1992) Implications of epidermal growth factor (EGF) induced EGF receptor aggregation. Biophys. J. **63**, 98–110
8 Wiley, H. S. (1988) Anomalous binding of epidermal growth factor to A431 cells is due to the effect of high receptor densities and a saturable endocytic system. J. Cell Biol. **107**, 801–810
9 Chamberlin, S. G. and Davies, D. E. (1998) A unified model of c-erbB receptor homo- and heterodimerisation. Biochim. Biophys. Acta **1384**, 223–232
10 Livneh, E., Prywes, R., Kashles, O., Reiss, N., Sasson, I., Mory, Y., Ullrich, A. and Schlessinger, J. (1986) Reconstitution of human epidermal growth factor receptors and its deletion mutants in cultured hamster cells. J. Biol. Chem. **261**, 12490–12497
11 van Belzen, N., Spaargaren, M., Verkleij, A. J. and Boonstra, J. (1990) Interaction of epidermal growth factor receptors with the cytoskeleton is related to receptor clustering. J. Cell. Physiol. **145**, 365–375
12 van der Heyden, M. A. G., Nievers, M., Verkleij, A. J., Boonstra, J. and van Bergen en Henegouwen, P. M. P. (1997) Identification of an intracellular domain of the EGF receptor required for high-affinity binding of EGF. FEBS Lett. **410**, 265–268
13 Bowen, S., Stanley, K., Selva, E. and Davis, R. J. (1991) Constitutive phosphorylation of the epidermal growth factor receptor blocks mitogenic signal transduction. J. Biol. Chem. **266**, 1162–1169
14 Davis, R. J. (1988) Independent mechanisms account for the regulation of protein kinase C of the epidermal growth factor receptor affinity and tyrosine-protein kinase activity. J. Biol. Chem. **263**, 9462–9469
15 Countaway, J. L., Gironès, N. and Davis, R. J. (1989) Reconstruction of epidermal growth factor receptor transmodulation by platelet-derived growth factor in Chinese hamster ovary cells. J. Biol. Chem. **264**, 13642–13647
16 Roy, L. M., Gittinger, C. K. and Landreth, G. E. (1989) Characterization of the epidermal growth factor receptor associated with cytoskeletons of A431 cells. J. Cell. Physiol. **140**, 295–304
17 van Bergen en Henegouwen, P. M. P., Defize, L. H. K., de Kroon, J., van Damme, H., Verkleij, A. J. and Boonstra, J. (1989) Ligand-induced association of epidermal growth factor receptor to the cytoskeleton of A431 cells. J. Cell. Biochem. **39**, 455–465
18 Weigant, F. A. C., Blok, F. J., Defize, L. H. K., Linnemans, W. A. M., Verkleij, A. J. and Boonstra, J. (1986) Epidermal growth factor receptors associated to cytoskeletal elements of epidermal carcinoma (A431) cells. J. Cell Biol. **103**, 87–94
19 McClure, S. J. and Robinson, P. J. (1996) Dynamin, endocytosis and intracellular signalling. Mol. Membr. Biol. **13**, 189–215
20 Ringerike, T., Stang, E., Johannessen, L. E., Sandnes, D., Levy, F. O. and Madshus, I. H. (1998) High-affinity binding of epidermal growth factor (EGF) to EGF receptor is disrupted by overexpression of mutant dynamin (K44A). J. Biol. Chem. **273**, 16639–16642
21 Walker, F. and Burgess, A. W. (1991) Reconstitution of the high affinity epidermal growth factor receptor on cell-free membranes after transmodulation by platelet-derived growth factor. J. Biol. Chem. **266**, 2746–2752
22 Walton, G. M., Chen, W. S., Rosenfeld, M. G. and Gill, G. N. (1990) Analysis of deletions of the carboxyl terminus of the epidermal growth factor receptor reveals self-phosphorylation at tyrosine 992 and enhanced *in vivo* tyrosine phosphorylation of cell substrates. J. Biol. Chem. **265**, 1750–1754
23 den Hartigh, J. C., van Bergen en Henegouwen, P. M. P., Verkleij, A. J. and Boonstra, J. (1992) The EGF receptor is an actin-binding protein. J. Cell Biol. **119**, 349–355
24 Sorkin, A., Mazzotti, M., Sorkin, T., Scotto, L. and Beguinot, L. (1996) Epidermal growth factor receptor interaction with clathrin adaptors is mediated by the Tyr^{654}-containing internalization motif. J. Biol. Chem. **271**, 13377–13384
25 Chang, C.-P., Lazar, C. S., Walsh, B. J., Komuro, M., Collawn, J. F., Kuhn, L. A., Tainer, J. A., Trowbridge, I. S., Farquhar, M. G., Rosenfeld, M. G. et al. (1993) Ligand-induced internalization of the epidermal growth factor receptor is mediated by multiple endocytic codes analogous to the tyrosine motif found in constitutively internalized receptors. J. Biol. Chem. **268**, 19312–19320
26 Chen, W. S., Lazar, C. S., Lund, K. A., Welsh, J. B., Chang, C.-P., Walton, G. M., Der, C. J., Wiley, H. S., Gill, G. N. and Rosenfeld, M. G. (1989) Functional independence of the epidermal growth factor receptor from a domain required for ligand-induced internalization and calcium regulation. Cell **59**, 33–43
27 Holbrook, M. R., O'Donnell, Jr, J. B., Slakey, L. L. and Gross, D. J. (1999) Epidermal growth factor receptor internalization rate is regulated by negative charges near the SH2 binding site Tyr992. Biochemistry **38**, 9348–9356
28 Mayo, K. H., Nunez, M., Burke, C., Starbuck, C., Lauffenburger, D. and Savage, Jr, C. R. (1989) Epidermal growth factor receptor binding is not a simple one-step process. J. Biol. Chem. **264**, 17838–17844
29 Chung, J. C., Sciaky, N. and Gross, D. J. (1997) Heterogeneity of epidermal growth factor binding kinetics on individual cells. Biophys. J. **73**, 1089–1102
30 Berkers, J. A. M., van Bergen en Henegouwen, P. M. P. and Boonstra, J. (1991) Three classes of epidermal growth factor receptor on HeLa cells. J. Biol. Chem. **266**, 922–927

Received 30 May 2000/27 July 2000; accepted 1 September 2000